

THE NUMERICAL AND EXPERIMENTAL TESTING OF AXISYMETRIC MODEL FLOW

UDC 532.51

Slavica Ristić, Dušan Matić, Aleksandar Vitić, Marija Samardžić

Military Technical Institute (MTI), Belgrade, Serbia

Abstract. *The test of the flow around axisymmetrical model was performed in the wind tunnel for Mach number $M^\infty = 0.3$. The aerodynamic forces and moments were measured by the six-component internal strain gage balance. Oil emulsion film was used for flow visualization in the boundary layer.*

The basic goal of the test was to provide reliable experimental data for the purpose of uncertainty analysis of numerical results. Drag coefficients, lift coefficients and flow pattern obtained by numerical simulation, show a good agreement with experimental results.

Key words: *wind tunnel, aerodynamic forces and moments, axisymmetrical model, boundary layer, flow visualization, numerical simulation*

1. INTRODUCTION

The modern design process of aircrafts and missiles needs the use of a variety of theoretical, experimental and numerical methods. The experimental methods mostly used are: measuring of the aerodynamic forces and moments on the model in wind tunnels, measuring of the pressure distribution on the model surface and visualization of the flow around the model in wind tunnels or around real aircraft in free flight [1,5,7-10]. Computational Fluid Dynamics (CFD) has already demonstrated its capability to produce solutions of various very complex flows. The development of methods for the uncertainty analysis (verification and validation) of the numerical flow simulations results is not possible without comparison of numerical and experimental results. Good agreement shows good quality of the numerical simulation [2-4,6].

The results for the aerodynamic coefficients and flow pattern in the boundary layer around the axisymmetrical body are shown in this article. The measurement of the aerodynamic forces and moments by six-component internal strain gage balance VTI38A and the visualization of the flow with oil emulsion film were performed in the MTI trisonic wind tunnel, for speed of undisturbed flow with Mach number $M_\infty = 0.3$ and the angles of attack of the model in the range from $\alpha = -2^\circ$ to $+18^\circ$ [10].

Fluent 6.1 was used for numerical simulations of the turbulent flow around the tested model. Numerical simulations were performed for a wide range of Reynolds numbers and

angles of attack of the body, for seawater and air. Only a part of results, which concerns the numerical simulations of the flow with air, for experiment in the wind tunnel, is shown in this article [6].

2. THE DESCRIPTION OF THE MODEL AND TEST EQUIPEMENT

The wind tunnel T-38 in MTI, where the experiments were performed, is a blow-down, pressurized wind tunnel, with 1.5x1.5m, square test section. Mach numbers in range from $M_\infty=0.2$ to 4.0 can be achieved in test section, with Reynolds numbers up to 110 millions per meter [8,10]. A test section for subsonic and supersonic flows has solid walls, for transonic flows porous walls. Depending of M_∞ , wall porosity varies between 1.5% and 8 %. The run times of experiments in the tunnel can vary from 6 to 60 seconds, corresponding to stagnation pressure P_0 and M_∞ .

The aluminum alloy and steel were used for model fabrication. The length of the model is 967 mm and its diameter is 66.6 mm. The model was fixed to the angle of attack change mechanism, specially designed 15° adapter and 15° bent sting, with the pitch angle in range from -4° to $+25^\circ$, for the roll angle of 0° by this mechanism [8-10].



Fig. 1. –Model in the wind tunnel

A very precise six-component strain gage balance VTI38A was put inside of the model, for the purpose of measuring aerodynamic forces and moments. The range of the balance is 3000 N for the normal force, 3000 N for the side force, 700 N for the axial force, and 300 Nm for the pitching moment and 50 for the rolling moment. The accuracy of the balance is approximately 0.3% FS. Balance was calibrated before the measuring. It was set on the 50 mm diameter sting.

The model was painted in black to provide maximal visibility of the flow visualization effects. [1,5,8,9].

3. THE DESCRIPTION OF THE EXPERIMENT

3.1. The measuring of the aerodynamic coefficients

The experiment data acquisition system in the wind tunnel consisted of 64 – channel Teledyne system controlled by Compaq PC. 16-bit A/D converter (accuracy 0.1 PS of channels) digitalized data from all analogous channels. The sampling rate was 200 sam-

ples per second. The digital data were received by Digital ALFA SERVER and written to the disc for further processing. Data processing was performed by standard software [10].

Mach and Reynolds numbers in the test section of the wind tunnel were determined by measuring of the stagnation pressure P_0 and stagnation temperature T_0 in the settling chamber and static pressure P_{st} in the test section of the wind tunnel. Two coordinate systems were used during data processing: wind tunnel (relative) and aerodynamic coordinate system.

3.2. The visualization of the flow in the boundary layer

Oil emulsion films based on the petroleum, oleic acid and titanium dioxide (TiO_2) powder were used for visualization of the flow in the model boundary layer. Two techniques of oil film emulsion depositing were used: the continual layer on the one side (deposited by fine sponge), and dots on the other one (deposited by fine soft brush immediately before blowdown). [1,5,8].

The model was removed out of the test section after each blow down, for the purpose of taking pictures of it, by Canon A70 digital camera.

4. THE NUMERICAL SIMULATION OF THE FLOW

Unigraphics 18.0 was used for modeling body with axysymmetrical geometry. The geometry of the body was exported to Gambit 2.0, software for basic geometry modeling and computational grid generation. [3-4,6].

The computational space had a cylinder shape. Distance from the inlet boundary of the computational space to the body was equal to 0.5, and from the outlet boundary was equal to 2.5 of the body length. The distance from the body to the symmetry boundary of the computational space was bigger than 5 diameters of the body.

The tetrahedral hybrid unstructured computational grid with variable density was generated inside of the computational space for each angle of attack of the body separately. The appropriate hexahedral grid for boundary layer was generated in the vicinity of the body. Depending on the body angle of attack, the number of elements in the computational grids was varied in the range from 348 000 to 386 000 (number of elements increases as the angle of attack of the body increases). The average value of the local Reynolds number y^+ was in the range from 40 to 48, depending on body angle of attack. Maximal value of y^+ was in the range from 60 to 71.

Fluent 6.1 was used for numerical simulation of the flow around the axysymmetrical body. Solutions for Navier–Stokes equations were obtained by using of Reynolds Average Solutions technique (RANS). The segregated numerical scheme was used to obtain the solution of the flow. The flow was considered as steady.

Two turbulence models $k - \varepsilon$ RNG and $k - \omega$ standard models for turbulent stresses were used. The standard wall functions were used in the area of boundary layer. For pressure and velocity fields coupling, SIMPLE algorithm was selected. Boundary conditions for numerical simulation of the flow were the same as the conditions in the wind tunnel during the experiment.

The converged solutions for integral quantities of interest were obtained after about 250 iterations. The solution convergence criterion for all calculations was based on the scaled sum of the mass residuals. The value of $1 \cdot 10^{-4}$ was enough to obtain convergence of all flow parameters of interest, primarily resistance coefficient and lift coefficient [3,6].

5. THE ANALYSIS OF THE RESULTS

5.1. The analysis of aerodynamic coefficients

The results for two aerodynamic coefficients drag coefficient C_x and lift coefficient C_z , obtained by the experiment in the wind tunnel and by the numerical simulations of the flow, are shown in Figures 2. and 3, as a function of the angle of attack.

The diagram given in figure 2 shows good agreement between numerical simulations of the flow and experimental results, for both used turbulence models, in the range of the angles of attack of the body from 2° to 8° . For angles bigger than 8° , C_x values obtained with the use of $k - \varepsilon$ RNG turbulence model are still in good agreement with experimental values (up to 4% difference), while the difference between C_x values obtained with the use of $k - \omega$ standard turbulence model and experimental values increase as the angle of attack increases.

The diagram given in fig. 3 shows that agreement between values of numerical lift coefficient C_z and experimental ones are not as good as they were for drag coefficient C_x . The difference is almost equal for both used turbulence models in the range of small angles of attack. For angles bigger than $\alpha = 6^\circ$, the difference between C_z obtained with the $k - \varepsilon$ RNG turbulence model and experimental values decrease as the angle of attack increases (6.4% for $\alpha = 18^\circ$). Differences between C_z values obtained with the use of $k - \omega$ standard turbulence model and experimental values for angles of attack bigger than 6° are almost equal as they are for $\alpha = 6^\circ$.

There are two basic reasons for differences between experimental and numerical values: the simplifications introduced in the experimental setup and in the geometry of the computational space. In the experimental setup, the influence of the model support sting was neglected. On the other hand, during the generation of computational space and grid, the model support sting was not modeled [8].

From the results presented in figure 3, it can be concluded that the influence of the lift force generated on the model support sting on the lift coefficient C_z is not negligible for a whole range of tested angles of attack of the model. Influence of a generated axial force on the drag coefficient C_x is smaller and limited to the angles of attack bigger than 8° (figure 2).

The second reason is that measured values of resistance and lift forces for small angles of attack of the model (α up to 4°) were too small compared to the measuring range of the used balance and its accuracy level [8-10]. The agreement between numerical and experimental results was much better when $k - \varepsilon$ RNG turbulence model was used, which is in accordance with the former author experience with the numerical simulations. Nevertheless, convergence of integral quantities of interest was faster when $k - \omega$ standard turbulence model was used.

There are considerable differences between numerical results obtained by the use of different turbulence models. For the drag coefficient C_x , bigger differences emerge when the angle of attack of the body is bigger than 10° . The situation is similar for the lift coefficient C_z . These differences are unexpected and need further study.

For the purpose of uncertainty analysis of the drag coefficient C_x , experimental values corresponding to the angles of attack of the body bigger than 4° can be used, because for these angles, simplifications introduced in the experiment setup and accuracy level of the balance do not have big influence on experimental values of C_x .

5.2. The Analysis of the flow visualization results

The flow patterns on the body surface were presented for all the angles of attack of the body for which the flow was numerically simulated, i.e. $\alpha = 0^\circ - 18^\circ$, with 2° step. The analysis of the photos (fig 4-7) shows that the effects of the flow visualization after 45 seconds wind tunnel run are very good, because there was enough time to develop flow pattern.

Figures of the whole model, were taken in purpose to compare experimental flow patterns with flow patterns obtained by numerical simulations of the flow. The analysis of photographs show an excellent agreement of flow patterns obtained by the experiment and the numerical simulations. Certain differences are visible in the area behind the model support sting and in its immediate vicinity because this sting is not included in numerical model (figures 5a and 6a). Those differences are small, which shows that modified 15° adapter causes small disturbances in the flow. [8,10].

The photographs of experimental flow patterns and numerical simulations flow patterns show that the comparison of flow patterns is easier when oil emulsion is deposited in dots over the surface of the model. As the body during the process of flow pattern generation in Fluent is considered as transparent, some overlapping of the flow patterns in the figures occurs which complicates comparison with the experimentally flow patterns.

6. CONCLUSION

The main goal of the experiment, to provide reliable experimental data for the purpose of uncertainty analysis of the numerical simulation results has been accomplished. For the purpose of uncertainty analysis the experimental values for the drag coefficient C_x are used. The differences between the experimental and numerical results are caused by simplifications that were introduced in the experiment setup and in numerical model, and because of the accuracy level of the used balance [6,8-10].

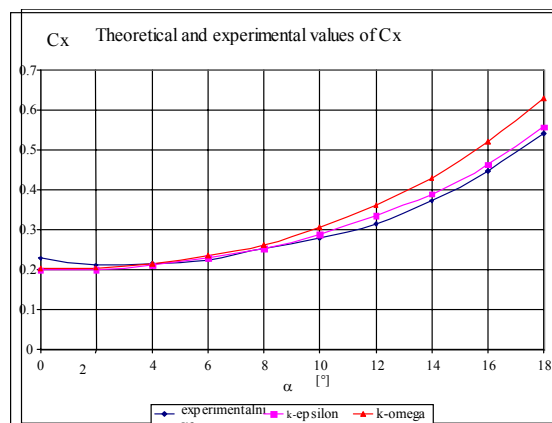


Fig. 2. – Diagram of the drag coefficient C_x as a function of the angle of attack

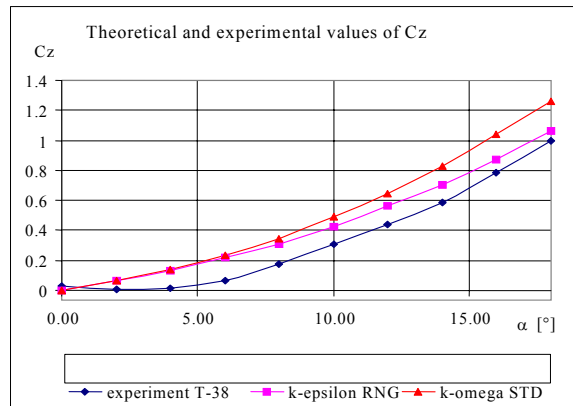
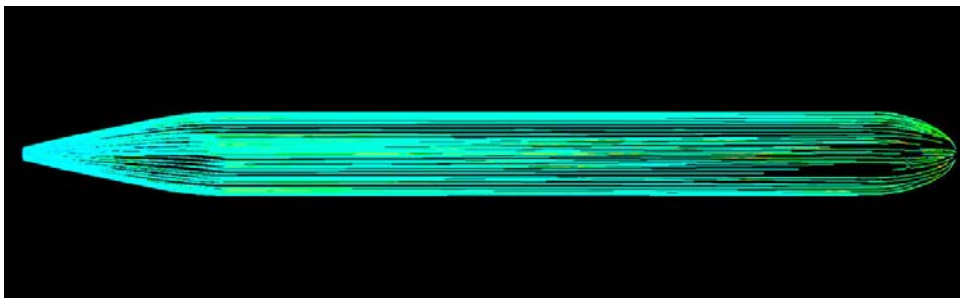


Fig. 3. - Diagram of the lift coefficient C_z as a function of the angle of attack

The visualization of the flow in the boundary layer by the oil emulsion films appears as good choice. The experiments with oil films visualization of the flow should be performed when ambience temperature is over 20°C if it is possible because the blow down time will be much shorter and the flow patterns on the model surface are much better defined.



a)



b)

Fig. 4. Flow patterns on the model (experiment a) and numerical b)), $M_\infty = 0.3$, $\alpha = 0^\circ$

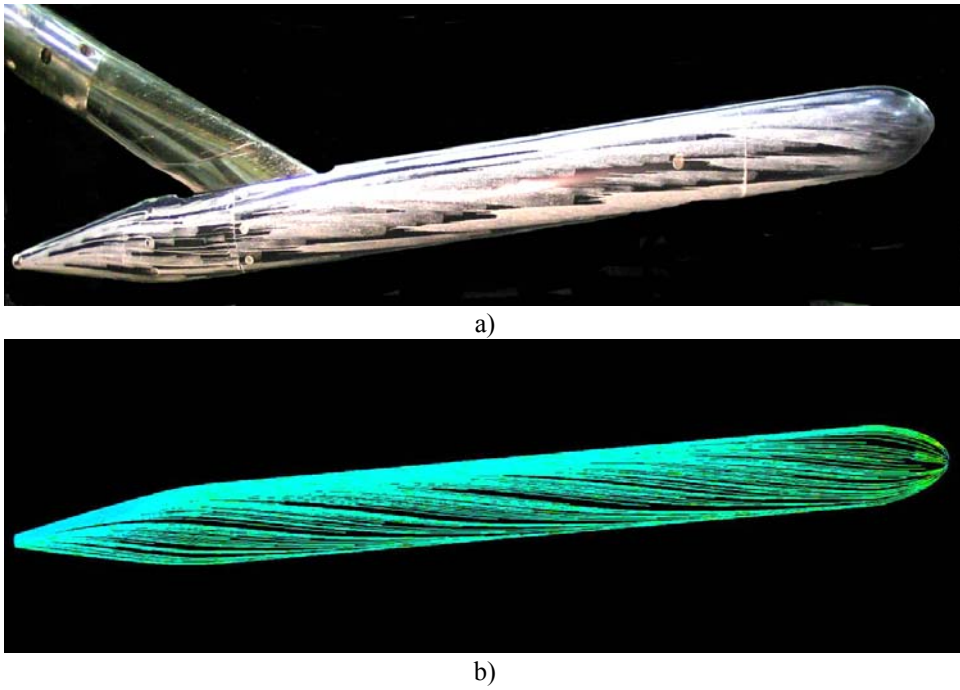


Fig. 5. - Experimental and numerical flow patterns on the model, $M_\infty = 0.3$ and $\alpha = 4^\circ$.

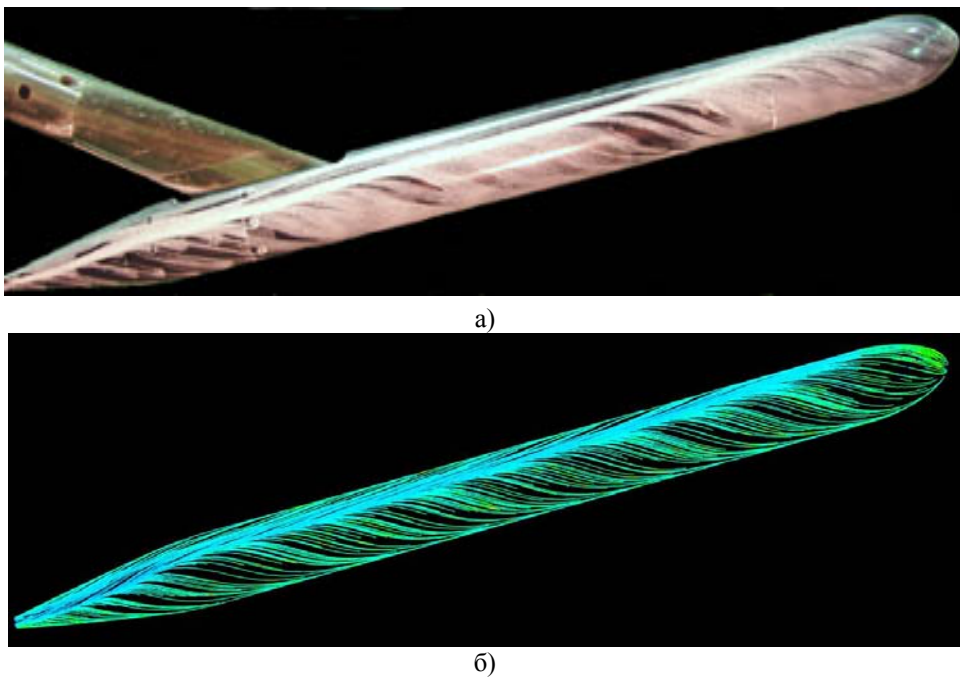


Fig. 6. - Flow pattern on the model for $M_\infty = 0.3$ and $\alpha = 14^\circ$ (side view).

Good agreement of flow patterns obtained by the experiment and by numerical simulation of the flow confirms the capability of used numerical technique. This experiment and available literature [1,5,8,9] show that methods of visualization are very useful for experiments that were performed in wind tunnels and for confirmation of the results that were obtained by numerical simulations.

REFERENCES

1. Marzkirch W. , 1977, Flow visualization, New York, Academic Press
2. Ferziger J.N. Perić M. , 1997, Computational Methods for Fluid Dynamics, Berlin, Springer
3. Roe P.L. (1982) Numerical Methods in Aeronautical Fluid Dynamics, London, Academic Press
4. Versteeg N.K. Malalasekera W. (1996) An Introduction to computational fluid dynamics-The finite volume method, London, Longman
5. Ristic S. (1999) The survey of the flow visualization methods in the wind tunnels, Belgrade, MTI
6. Matic D., 2005, Numerical Flow Simulation Around Rotational Model, Belgrade,MTI,
7. Pagendarm H.-G. and F.H. Post., 1995, Comparative visualization – approaches and examples, H. Müller, and B. Urban, editors, *Visualization in Scientific Computing*, Springer, Wien, pp., 95–108.,
8. Ristic S., Vitic A., Anastasijevic Z., Vukovic Đ., 2004, Investigation of Support Interaction Upon Aerodynamic Characteristics of a Torpedo Model in the T-38 Wind Tunnel, Scientific Technical Review, MTI, vol.44 no.1, pp. 50-57
9. Ristic S, Matic D., Vitic A., 2004, Visualization and numerical Simulation of the flow around the nose of the torpedo model, Proceedings of HIPNEF 2004, University of Nis, pp.267-273
10. Vitic A. (2003) Tests of the model torpedo for Mach number $M=0,3$ in the wind tunnel T 38, internal report, Belgrade, MTI

NUMERIČKO I EKSPERIMENTALNO ISPITIVANJE STRUJANJA OKO OSNOSIMETRIČNOG MODELA

Slavica Ristić, Dušan Matić, Aleksandar Vitić, Marija Samardjić

Ispitivanje strujanja oko osnosimetričnog modela je sprovedeno u aerotunelu za Mahov broj $M^\infty = 0.3$. Aerodinamičke sile i momenti su mereni šestokomponentnom unutrašnjom aerovagom. Vizualizacija strujanja u graničnom sloju je izvršena pomoću uljanih premaza. Osnovni cilj ispitivanja je bio da obezbedi validne eksperimentalne rezultate pomoću kojih će se vršiti analiza pouzdanosti numeričkih rezultata. Koeficijent otpora, koeficijent uzgona i strujne linije, dobijene numerički pokazuju odlično slaganje sa eksperimentalnim rezultatima.

Ključne reči: *Aerotunel, aerodinamičke sile i momenti, osnosimetrični model, granični sloj, vizualizacija strujanja, numerička simulacija*